

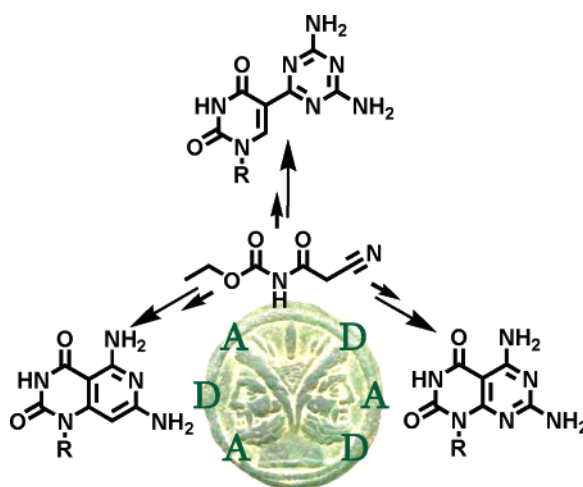
Janus-AT Bases: Synthesis, Self-Assembly, and Solid State Structures

Ali Asadi, Brian O. Patrick, and David M. Perrin*

Department of Chemistry, University of British Columbia, 2036 Main Mall,
Vancouver, British Columbia V6T-1Z1

dperrin@chem.ubc.ca

Received September 6, 2006



JANUS-AT HETEROCYCLES

The high yielding synthesis of heterocycles with defined H-bond accepting and donating capabilities provides for the design of self-assembling structures and specific recognition of biological targets. Herein we report the syntheses and solid-state structures of three self-complementary uracil/thymine derivatives where each presents the standard ADA face inherently complementary to adenine and a synthetically appended DAD face complementary to uracil/thymine. These heterocycles, which have never before been reported or characterized, represent diaminopurine–uracil/thymine hybrids that, in two of the three cases, relate to previously reported heterocyclic hybrids of G and C. All three heterocycles crystallized to afford the first X-ray crystal structures of self-complementary heterocycles capable of ADA–DAD pairing. The potential use in DNA and RNA recognition are briefly discussed.

Introduction

Whereas the specificity characteristic of life in an aqueous world is often attributed to hydrogen bonding, water effectively competes for hydrogen bonds. Thus the specificity of interactions attributed to H-bonding is further mediated by a delicate interplay between hydrophobic forces and electrostatic interactions. Such an interplay is typified in nucleic acids, wherein correct H-bonding along with hydrophobic base stacking and electrostatic interactions between phosphates and counterions ensures sequence specificity for complementary hybridization

and a semiconservative templated synthesis of DNA and RNA. Furthermore, nucleic acids associate into various regular supramolecular architectures including double and triple helices, G-quartets, and i-motifs which may compete with the standard double helical structure.¹

Synthesis of unnatural molecules capable of defined H-bonding interactions has led to the creation of artificial self-assembling structures and more recently supramolecular non-covalent polymers that have potential applications in nanotechnology,

(1) Lane, A. N.; Jenkins, T. C. *Curr. Org. Chem.* **2001**, *5*, 845–869.

molecular tectonics, and crystal engineering, particularly in organic media where H-bonding is considerably stronger, and in the solid phase where X-ray diffraction provides visualization of H-bonded arrays.^{2–10}

Although H-bond mediated assembly of two different monomers presenting complementary recognition sites (e.g., melamine and cyanuric or barbituric acid) has been used extensively to create a variety of architectures,^{11–28} there are far fewer antecedent examples in which self-complementary monomers have been examined for self-assembly.^{29–36} The consequence of monomeric self-complementarity affords the possibility of several multimeric material forms including trimers,^{35,37}

rosettes,^{26,30–32,38} regular noncovalent polymer arrays,^{4,5} and irregular crinkled heteromorphic composites.^{18,39–42}

When self-complementary monomers are designed to be simultaneously complementary to two nucleobases capable of Watson–Crick base pairing (i.e., G and C, or A and T), there is the intriguing potential for sequence specific DNA recognition that would compete with self-association. Such monomers have been nicknamed Janus-bases after the two-faced Roman god.⁴³ Nevertheless, the first example of such a J-base was actually a non-self-complementary pyrimidine (a J_{GA}-base) that that had been designed to simultaneously recognize C and U, which neither form a Watson–Crick base pair, nor readily associate in solution. Consequently, the simultaneous association of the J_{GA}-base with both C and U could be cleanly monitored by ¹H NMR titration that gave rise to new peaks which demonstrated the expected three-way interaction.^{43,44} Recently, the same J_{GA}-base was incorporated onto an octameric PNA homopolymer third strand that afforded recognition of heteroduplex DNA containing C–T mismatches.⁴⁵

Although there have been several reports on the synthesis and self-assembly of several classes of J_{GC}-bases which self-associate via a DDA–AAD interaction, and which could potentially recognize a G–C base pair,^{30–32,35,45} a solution-phase ¹H NMR experiment that could demonstrate simultaneous recognition of C and G by a J_{GC}-base, analogous to that which was used to demonstrate C and U recognition by the J_{GA}-base, would be difficult if not impossible to perform cleanly, and to date no such experiment has been reported. To date, these J_{GC}-heterocycles have been characterized by various techniques that verify only self-association whereas the potential for DNA recognition has remained entirely unexplored.

In order to eventually use J-bases to recognize both bona fide Watson–Crick base pairs, i.e., GC and AT, in contrast to various mismatches, one would need J_{AT}-bases in addition to the aforementioned J_{GC}-bases. Surprisingly, the synthesis of a J_{AT}-base has never been reported, either with an eye to DNA recognition, or more simply, in terms of an investigation of self-association via potential DAD–ADA H-bonding interactions.⁴⁶ Herein, we describe the design, high yielding syntheses, and, to the best of our knowledge, the first X-ray structures of solid-state supramolecular arrays of three J_{AT}-bases capable of DAD–ADA interactions (technically these are not AT-hybrids but closer to a thymine–diaminopurine or a uracil–diaminopurine hybrid). The monomers are shown in Figure 1. Several

(2) Brunsveld, L.; Folmer, B.; Meijer, E.; Sijbesma, R. *Chem. Rev.* **2001**, *101*, 4071–4097.

(3) Fournier, J.; Maris, T.; Wuest, J. *J. Org. Chem.* **2004**, *69*, 1762–1775.

(4) Gong, H.; Krische, M. *J. Am. Chem. Soc.* **2005**, *127*, 1719–1725.

(5) Ikeda, M.; Nobori, T.; Schmutz, M.; Lehn, J. *Chem.–Eur. J.* **2005**, *11*, 662–668.

(6) Laliberte, D.; Maris, T.; Wuest, J. *J. Org. Chem.* **2004**, *69*, 1776–1787.

(7) Steiner, T. *Angew. Chem.* **2002**, *41*, 48–76.

(8) Su, D.; Wang, X.; Simard, M.; Wuest, J. *Supramol. Chem.* **1995**, *6*, 171–178.

(9) ten Cate, A.; Kooijman, H.; Spek, A.; Sijbesma, R.; Meijer, E. *J. Am. Chem. Soc.* **2004**, *126*, 3801–3808.

(10) Lawrence, D. S.; Jiang, T.; Levett, M. *Chem. Rev.* **1995**, *95*, 2229–2260.

(11) Archer, E.; Goldberg, N.; Lynch, V.; Krische, M. *J. Am. Chem. Soc.* **2000**, *122*, 5006–5007.

(12) Archer, E.; Krische, M. *J. Am. Chem. Soc.* **2002**, *124*, 5074–5083.

(13) Arduini, M.; Crego-Calama, M.; Timmerman, P.; Reinhoudt, D. *J. Org. Chem.* **2003**, *68*, 1097–1106.

(14) Beijer, F.; Sijbesma, R.; Vekemans, J.; Meijer, E.; Kooijman, H.; Spek, A. *J. Org. Chem.* **1996**, *61*, 6371–6380.

(15) Bernhardt, P. *Inorg. Chem.* **1999**, *38*, 3481–3483.

(16) Binder, W. *Monatsh. Chem.* **2005**, *136*, 1–19.

(17) Klok, H.; Jolliffe, K.; Schauer, C.; Prins, L.; Spatz, J.; Moller, M.; Timmerman, P.; Reinhoudt, D. *J. Am. Chem. Soc.* **1999**, *121*, 7154–7155.

(18) Mascal, M.; Hansen, J.; Fallon, P.; Blake, A.; Heywood, B.; Moore, M.; Turkenburg, J. *Chem.–Eur. J.* **1999**, *5*, 381–384.

(19) Murray, T. J.; Zimmerman, S. C. *J. Am. Chem. Soc.* **1992**, *114*, 4010–4011.

(20) Perdigao, L.; Champness, N.; Beton, P. *Chem. Commun.* **2006**, 538–540.

(21) Scherman, O.; Ligthart, G.; Sijbesma, R.; Meijer, E. *Angew. Chem.* **2006**, *45*, 2072–2076.

(22) Sessler, J. L.; Wang, R. Z. *J. Org. Chem.* **1998**, *63*, 4079–4091.

(23) Seto, C. T.; Whitesides, G. M. *J. Am. Chem. Soc.* **1991**, *113*, 712–713.

(24) Thalacker, C.; Miura, A.; De Feyter, S.; De Schryver, F.; Wurthner, F. *Org. Biomol. Chem.* **2005**, *3*, 414–422.

(25) Yagai, S.; Nakajima, T.; Karatsu, T.; Saitow, K.; Kitamura, A. *J. Am. Chem. Soc.* **2004**, *126*, 11500–11508.

(26) Zerkowski, J. A.; Seto, C. T.; Whitesides, G. M. *J. Am. Chem. Soc.* **1992**, *114*, 5473–5475.

(27) Zerkowski, J. A.; Seto, C. T.; Wierda, D. A.; Whitesides, G. M. *J. Am. Chem. Soc.* **1990**, *112*, 9025–9026.

(28) Zhang, X.; Chen, X. *Cryst. Growth Des.* **2005**, *5*, 617–622.

(29) Lehn, J. M.; Mascal, M.; Decian, A.; Fischer, J. *J. Chem. Soc., Perkin Trans. 2* **1992**, 461–467.

(30) Fenniri, H.; Mathivanan, P.; Vidale, K.; Sherman, D.; Hallenga, K.; Wood, K.; Stowell, J. *J. Am. Chem. Soc.* **2001**, *123*, 3854–3855.

(31) Mascal, M.; Hext, N.; Warmuth, R.; Arnall-Culliford, J.; Moore, M.; Turkenburg, J. *J. Org. Chem.* **1999**, *64*, 8479–8484.

(32) Mascal, M.; Hext, N. M.; Warmuth, R.; Moore, M. H.; Turkenburg, J. P. *Angew. Chem.* **1996**, *35*, 2204–2206.

(33) Nagai, K.; Hayakawa, K.; Ukai, S.; Kanematsu, K. *J. Org. Chem.* **1986**, *51*, 3931–3939.

(34) Schall, O. F.; Gokel, G. W. *J. Am. Chem. Soc.* **1994**, *116*, 6089–6100.

(35) Sessler, J.; Jayawickramarajah, J.; Sathiosatham, M.; Sherman, C.; Brodbelt, J. *Org. Lett.* **2003**, *5*, 2627–2630.

(36) Zhu, P.; Kang, H.; Facchetti, A.; Evmenenko, G.; Dutta, P.; Marks, T. *J. Am. Chem. Soc.* **2003**, *125*, 11496–11497.

(37) Zimmerman, S. C.; Duerr, B. F. *J. Org. Chem.* **1992**, *57*, 2215–2217.

(38) Kolotuchin, S.; Zimmerman, S. *J. Am. Chem. Soc.* **1998**, *120*, 9092–9093.

(39) Mathias, J. P.; Seto, C. T.; Simanek, E. E.; Whitesides, G. M. *J. Am. Chem. Soc.* **1994**, *116*, 1725–1736.

(40) Mathias, J. P.; Simanek, E. E.; Whitesides, G. M. *J. Am. Chem. Soc.* **1994**, *116*, 4326–4340.

(41) Mathias, J. P.; Simanek, E. E.; Zerkowski, J. A.; Seto, C. T.; Whitesides, G. M. *J. Am. Chem. Soc.* **1994**, *116*, 4316–4325.

(42) Zerkowski, J. A.; Seto, C. T.; Whitesides, G. M. *J. Am. Chem. Soc.* **1992**, *114*, 5473–5475.

(43) Branda, N.; Kurz, G.; Lehn, J. M. *Chem. Commun.* **1996**, 2443–2444.

(44) Marsh, A.; Nolen, E. G.; Gardinier, K. M.; Lehn, J. M. *Tetrahedron Lett.* **1994**, *35*, 397–400.

(45) Chen, D.; Meena; Sharma, S.; McLaughlin, L. *J. Am. Chem. Soc.* **2004**, *126*, 70–71.

(46) Zhu et al.³⁶ published on growth of thin films based on the self-assembly of 5-[4-[2-(4,6-diamino-[1,3,5]triazin-2-yl)-vinyl]-benzylidene]-pyrimidine-2,4,6-trione which presents a DAD face (diaminotriazine) along with two ADA faces (benzylidenebarbituric acid) that are separated by an extended styrenyl linker.

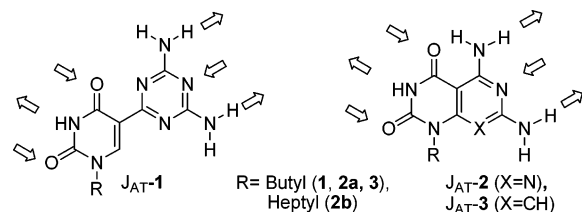


FIGURE 1. Janus-AT nucleobases **1**, **2a**, **2b**, **3**. Arrows indicate expected H-bond donating or accepting functionalities.

considerations arose with regards to the design of J_{AT-1} , J_{AT-2} , and J_{AT-3} as well as the choice for their corresponding synthetic routes. To begin with, we chose to incorporate a diaminopurine-like face instead of a more natural A-like (aminopurine) face to afford three H-bonds instead of two with the thymine-like face. Although the ADA–DAD hydrogen bonding array is not generally found in regular DNA base pairs, it exists in the cyanophage S-2L viral genome that contains 2,6-diaminopurine,⁴⁷ a base that has been found to increase duplex stability and specificity in synthetic systems relative to the more common adenine and thymine (A–T) base pair.⁴⁸ In addition, previous reports on ADA–DAD associated networks involving melamine guided our designs. From a synthetic perspective, heterocycles with two exocyclic amines, i.e., J_{AT-1} , J_{AT-2} , and J_{AT-3} , would be somewhat more synthetically accessible compared to analogues with only one exocyclic amine, particularly for the synthesis of J_{AT-1} (*vide infra*). J_{AT-1} was chosen for synthetic ease despite the considerable rotational flexibility between the two aryl rings. J_{AT-2} and J_{AT-3} were chosen because they are, respectively, constitutional isomers of the J_{GC} -base reported by both Lehn⁴⁹ and Fenniri³⁰ and of the J_{GC} -base reported by Mascali.^{31,32} Furthermore, the diaminopurine-like face in J_{AT-3} was installed on a pyridinyl ring system (as opposed to a pyrimidinyl ring system in J_{AT-2}) to afford the eventual possibility of regioselective attachment to a (deoxy)ribose moiety on either the nitrogen of the uracil-like face or on the carbon of the diaminopurine-like face. Finally, for the current study we chose high yielding synthetic routes that were amenable to extensive variation in terms of the alkyl chain that could be installed on either target, and three alkyl derivatives were studied in greater detail with regards to self-assembly.

Results

Synthesis of **1** (Scheme 1) began with the facile construction of 5-cyanouracil, **6**,⁵⁰ that was obtained from condensation of *N*-cyanoacetylurethane, **4**, with triethylorthoformate in acetic anhydride at reflux to afford **7** followed by addition of butylamine and ring closure reaction in water in high yield (94%). 5-Cyanouracil, **6**, was then condensed with dicyandiamide in dry DMSO in the presence of KOH at reflux to afford **1** in 80% yield.^{3,6}

The procedure for synthesizing **2a** and **2b** (Scheme 2) started with the condensation of *N*-cyanoacetylurethane, **4**, with carbon

disulfide^{51,52} in the presence of potassium carbonate in DMF, followed by treatment of the resulting ketene dithioacetal dipotassium salt, **7**, with 2 equiv of methyl iodide in water–acetonitrile to give ketene dithioacetal, **8**. Intermediates **9a** and **9b** were obtained via dropwise addition of appropriate amine to an ethanolic solution of **5** at room temperature to afford a presumed monoamine adduct that was cyclized at reflux to afford the 5-cyano-6-methylthiouracils **9a** and **9b** which were characterized by both ¹H/¹³C NMR and HRMS. In addition, **9a** was crystallized and characterized by X-ray diffraction to verify the correct substitution at positions 5 and 6 (Supporting Information). Compounds **9a** and **9b** were reacted with guanidine (free base generated *in situ*) in ethanol at reflux to afford the corresponding bicyclic products **2a** and **2b** in good to excellent yields.

The procedure for synthesizing **3** (Scheme 3) started with the condensation of *N*-cyanoacetylurethane, **4**, with triethyl orthoacetate in acetic anhydride at reflux to afford **10** followed by addition of butylamine and ring closure in water in high yield (91%). 6-Methyl 5-cyanouracil, **11**, was then condensed with carbon disulfide in dry THF in the presence of potassium *t*-butoxide at room temperature followed by acidic workup to afford **12** in 89% yield which was characterized by both ¹H/¹³C NMR and HRMS. In addition, **12** was crystallized in acetonitrile and characterized by X-ray diffraction to verify the formation of the novel structure. Compound **12** was treated with 30% ammonium hydroxide at reflux in a sealed tube to afford **13** in high yield (93%). A hexyl derivative of **13** was also synthesized similarly and characterized by X-ray diffraction (see Supporting Information). Intermediate **14** was obtained via dropwise addition of methyl iodide to an aqueous solution of **13** in the presence of NaOH at room temperature in high yield (90%). Oxidation of methyl sulfide **14** to methyl sulfone **15** was achieved through two routes; by using MCPBA in chloroform at room temperature, or by using hydrogen peroxide in formic acid at room temperature in high yields (95%). Compound **15** was reacted with ammonia in methanol at 100 °C in a sealed tube to afford the bicyclic product **3** in good yield.

In general terms, J_{AT-1} , J_{AT-2} , and J_{AT-3} represent three different, yet related, shape classes of self-complementary heterocycles whose synthetic elaboration, composition, and full characterization have heretofore been unknown. Compound **1** was moderately soluble (~12 mg/mL) in polar solvents (DMSO, DMF, NMP, methanol) that are known to disrupt hydrogen bonds whereas it was virtually insoluble in chloroform, dichloromethane, benzene, toluene, nitrobenzene, THF, or water. Compounds **2a** and **2b** were practically insoluble in conventional solvents and manifested low solubility even in DMSO, DMF, and NMP (<2 mg/mL) but readily dissolved in 98% formic acid to an appreciable extent. As our synthetic routes allowed us to prepare a series of alkyl derivatives, we undertook such in the hope of finding a well-behaved monomer whose self-association could be monitored in various NMR solvents such as CDCl₃ wherein H-bonding is observable and strong. Several other analogs of **1** (ethyl, propyl, phenyl, and hexadecyl) and of **2** (ethyl, propyl, pentyl, and hexyl) were prepared similarly (data not shown), and none was appreciably more soluble in

(47) Kirnos, M. D.; Khudyakov, I. Y.; Alexandrushkina, N. I.; Vanyushin, B. F. *Nature* **1977**, *270*, 369–370.

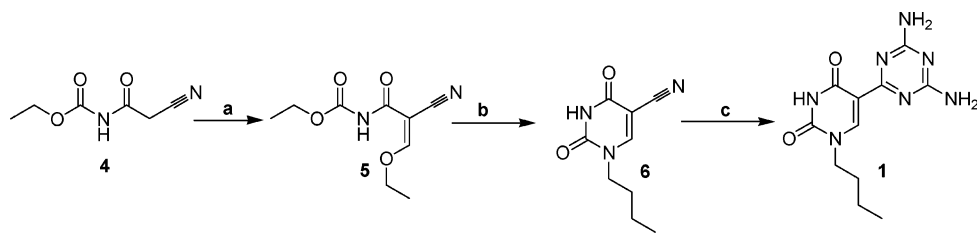
(48) Haaima, G.; Hansen, H.; Christensen, L.; Dahl, O.; Nielsen, P. *Nucleic Acids Res.* **1997**, *25*, 4639–4643.

(49) Marsh, A.; Silvestri, M.; Lehn, J. *Chem. Commun.* **1996**, 1527–1528.

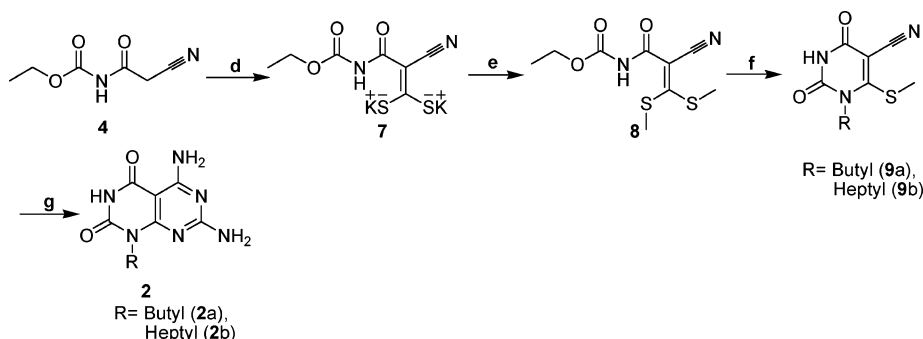
(50) Senda, S.; Hirota, K.; Notani, J. *Chem. Pharm. Bull.* **1972**, *20*, 1380–1388.

(51) Jensen, K. A.; Henrikse, L. *Acta Chem. Scand.* **1968**, *22*, 1107–1109.

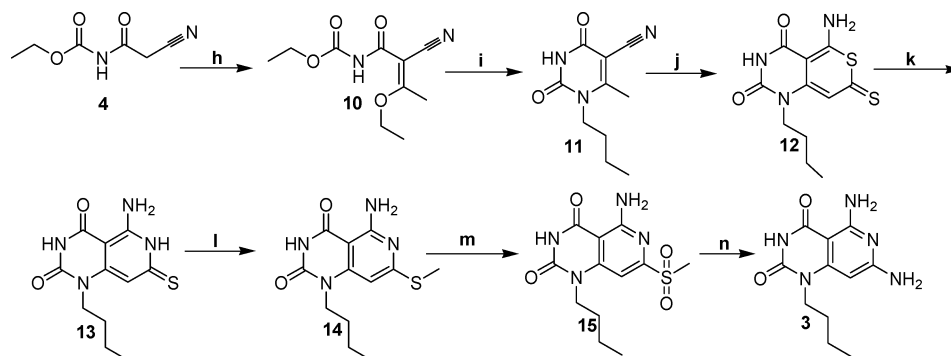
(52) Yokoyama, M.; Kumata, K.; Yamada, N.; Noro, H.; Sudo, Y. *J. Chem. Soc., Perkin Trans. 1* **1988**, 2309–2313.

SCHEME 1. Synthesis of J_{AT}-1

a) Triethylorthoformate, Acetic Anhydride, Reflux, 45 min, 95% b) Butyl amine, water, 85°C, 15 min, 93% c) dicyandiamide, KOH, DMSO, 95°C, 4 hours, 80 %

SCHEME 2. Synthesis of J_{AT}-2

d) CS₂, K₂CO₃, DMF, RT, 95% e) MeI, H₂O:CH₃CN (7:3), Reflux, 85% f) R-NH₂, EtOH, Reflux, 87 %
g) Guanidinium Hydrochloride, NaOEt, EtOH, Reflux, 85 %

SCHEME 3. Synthesis of J_{AT}-3

h) Triethyl orthoacetate, acetic anhydride, reflux, 40 min, 90 % i) Butylamine, H₂O, 20 min, 90 °C, 91%
j) i. *t*ButOK, dry THF, CS₂, RT, 2h ii. acetic acid, H₂O, 89% k) Ammonium hydroxide, sealed tube, 100 °C, 12 h, 93% l) MeI, NaOH, H₂O, 90% m) (H₂O₂, formic acid, 4 h, RT) or (MCPBA, CHCl₃, 4 h, RT), 95% n) NH₃, MeOH, Sealed tube, 100 °C, 24 h, 92%

any of the solvents noted. Therefore, this work features more in-depth studies on either butylated (**1**, **2a**, and **3**) or heptylated (**2b**) derivatives. Compound **3** was moderately soluble (~15 mg/mL) in polar solvents (DMSO, DMF, NMP, methanol) that are known to disrupt hydrogen bonds whereas it was virtually insoluble in chloroform, dichloromethane, benzene, toluene, nitrobenzene, THF, or water

Given the limited solubility of these compounds, we were unable to achieve suitably high concentrations in chloroform where H-bonds would have formed appreciably to be monitored by NMR.⁵³ That self-association in solution was unobservable

(53) We were unable to readily observe H-bonding by either UV-vis or ¹H NMR; consequently attempts to further assign the structure through ¹⁵N-¹H NMR experiments (e.g., flip-back ¹⁵N-¹H 2D-NOESY) failed to provide any meaningful information. Attempts to increase H-bond strength in *d*₆-DMSO by addition of CD₂Cl₂ or CDCl₃ also failed; even at 10% cosolvent, turbidity and ultimately precipitation prevailed before any new peaks characteristic of intermolecular H-bonds could be reliably observed.

is consistent with the finding that the ADA-DAD interaction is significantly weaker even in CHCl₃ ($K_a \sim 10^2 \text{ M}^{-1}$) than the DDA-AAD configuration ($K_a \sim 10^4 \text{ M}^{-1}$).¹⁹ Although H-bonding in general is considerably weaker in DMSO, the compounds were appreciably more soluble in DMSO compared to chloroform, and thus, their association was investigated by ¹H NMR. The ¹H chemical shifts of all three shape classes did not vary upon dilution from ~5 mg/mL down to 0.1 mg/mL in *d*₆-DMSO (see Supporting Information), and as such, we were unable to observe solution-phase self-association in a solvent from which H-bonded networks ultimately crystallized. Nevertheless, the inability to observe self-association in either chloroform or DMSO might also have been consistent with an incorrect supposition that we had prepared the said targets.

As all three syntheses began with creation of the uracil face prior to installation of the DAD face containing the two exocyclic amines, we were reasonably certain that we had indeed

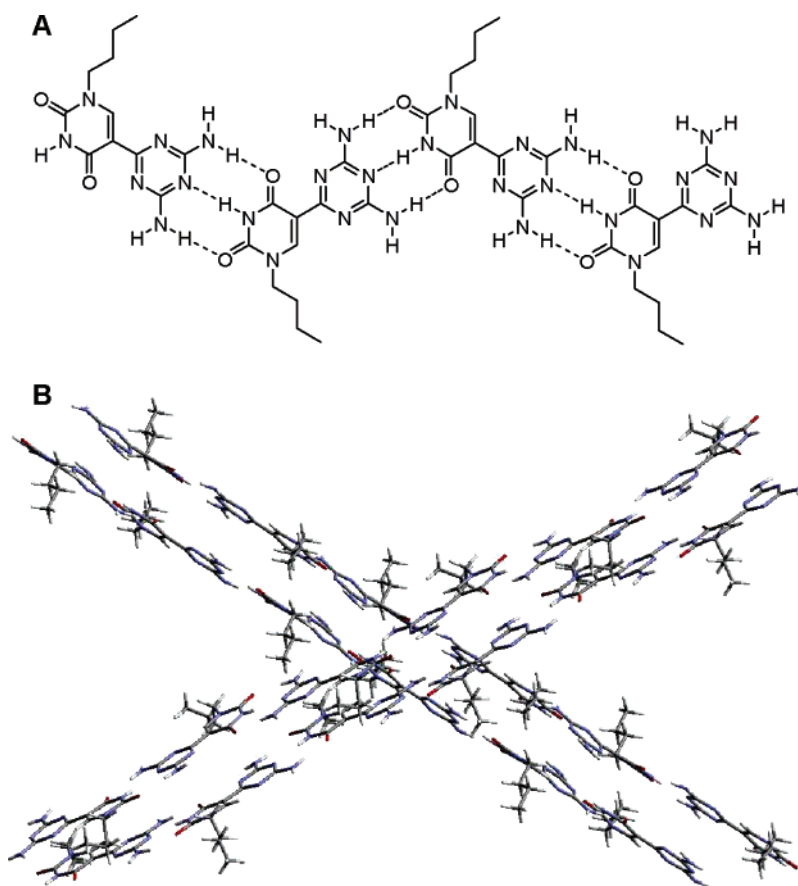


FIGURE 2. (A) Schematic of H-bonded ribbon array of J_{AT}-1. (B) Cut-away X-ray diffraction of the extended unit cell showing the lattice of 2 sets of parallel arrays.

prepared the target J_{AT}-bases as indicated. Nevertheless, neither ¹H NMR nor HRMS would unambiguously differentiate the intended J_{AT}-base from various constitutional isomers, including the corresponding J_{GC}-base. Although there was little likelihood of a rearrangement^{54–56} that would have transformed the intended J_{AT}-base target into any number of constitutional isomers, we sought additional confirmation of structure and thus turned to X-ray diffraction to provide unambiguous structural proof of compounds **1**, **2b**, and **3**. Beyond absolute proof of composition and connectivity, such structures would provide information as to whatever H-bonded associations these compounds would assume in the solid phase. One question we asked was whether these compounds would form hexameric rosettes as described for the J_{GC}-bases or extended arrays characteristic of melamine based materials.

For compound **1**, a single crystal suitable for X-ray diffraction was finally obtained by dissolving **1** in pure and very dry DMSO at elevated temperature whereupon after several days colorless prismatic crystals deposited after standing at room temperature. Crystals of **1** diffracted in a *P2*₁/*c* space group in which the asymmetric cell comprised four monomers and no solvent. The asymmetric cell was propagated using Mercury version 1.4.1 to identify a repeating matrix containing four slightly different H-bonded arrays of the type shown in Figure 2A,B.

Quite strikingly, the crystal packing of these arrays shows two repeating parallel arrays that are interdigitated with another

two parallel repeating arrays at an angle of approximately 60°. Two of the four arrays exhibit a dihedral angle between the two aromatic rings of approximately 5° with relatively coplanar H-bonds (Figure 3A) whereas the other two arrays exhibit a significant dihedral angle of nearly 20° (Figure 3B).

In one of the latter two arrays, a similar distortion angle is seen within the H-bonded faces (Figure 3C) where the three H-bonds deviate quite substantially from coplanarity. This structure nicely indicates the conformational flexibility of this biaryl J_{AT}-base as well as the extent to which the DAD–ADA H-bonding motif itself can vary in the same crystal structure. Similar variability in H-bonding is seen for Watson–Crick bases pairs within duplex B-DNA and is described as roll and propeller twist. To further demonstrate that the DAD and ADA faces remain in the intended tautomeric states in solution, a ¹⁵N–¹H HSQC NMR experiment was performed in *d*₆-DMSO on **1**. This demonstrated that two sets of two protons correlated with two nitrogens and not with three or four nitrogens, as would have been the case for other tautomers (see Supporting Information).

Attempts at obtaining single crystals of **2a** and **2b** for X-ray diffraction, in dry DMSO were unsuccessful as were numerous attempts with a variety of mixed solvents applied in conjunction with either vapor diffusion or refluxing at cloud point. Nevertheless, we were delighted to find that compound **2b** crystallized as colorless plates of two-component twin crystals via slow evaporation of a dilute solution of **2b** in 98% formic acid (**2a** also crystallized but provided twin crystals that did not cleanly diffract). X-ray diffraction identified a *P1* space group with a unit cell that comprised one molecule of **2b** and two molecules

(54) Graboyes, H.; Jaffe, G. E.; Pachter, I. J.; Rosenbloom, J. P.; Villani, A. J.; Wilson, J. W.; Weinstock, J. *J. Med. Chem.* **1968**, *11*, 568–573.

(55) Ueda, T.; Fox, J. J. *J. Org. Chem.* **1964**, *29*, 1762–1769.

(56) Ueda, T.; Fox, J. J. *J. Org. Chem.* **1964**, *29*, 1770–1772.

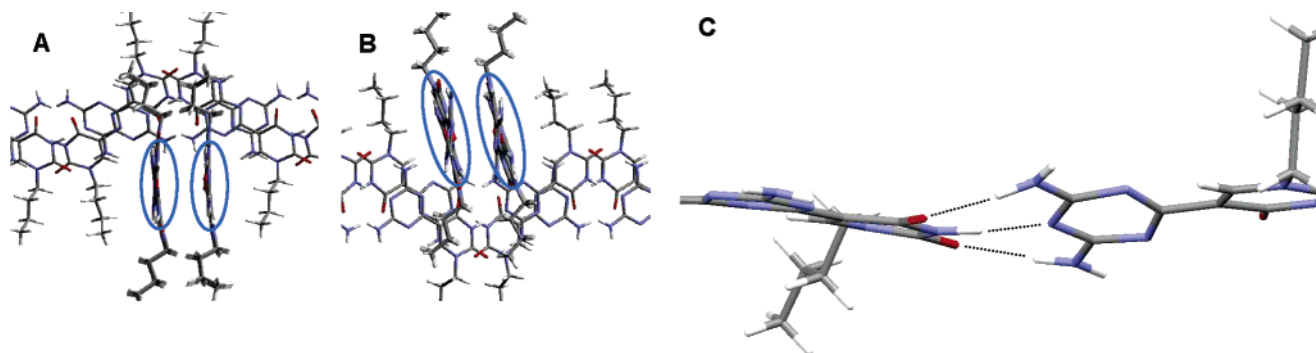


FIGURE 3. (A) Viewed along the array planes (blue ellipses), the dihedral angle of two arrays is roughly 5° or less. (B) The dihedral angle of the other two arrays is roughly 15°. (C) Shown is the propeller twist of a distorted DAD–ADA H-bonding interaction in one of the four arrays.

of formic acid. Extension of the unit cell indicated a formate-ion mediated cocrystal as shown in Figure 4A–C.

As can be seen in the X-ray crystal structure of **2b**, formic acid mediates the association by forming 3 complementary H-bonds within the polymeric array as it (1) protonates the DAD face, (2) accepts a proton from one of the exocyclic amines, and (3) intercepts the N₃H of the thymine-like face. The formate salt essentially masks the DAD face and provides for a DDD–AD pairing interaction with the thymine-like face. This unique asymmetrical hydrogen-bonding pattern between the pyrimidinium cation face and the thymine-like face mediated by formate anion, along with an AA H-bonding motif, gave rise to formation of an infinite hydrogen-bonded molecular ribbon lattice. In addition, a second molecule of formic acid serves to bridge one lattice with another.

As **2b** could only be crystallized from 98% formic acid (pH ~ 2), such acidic conditions obviated the possibility of observing the expected ADA–DAD interaction. In order to verify that **2b** indeed retained both the ADA and DAD faces in solution, we investigated its solution-phase tautomeric state. Thus, an ¹⁵N–¹H HSQC NMR experiment was performed in *d*₆-DMSO to demonstrate that, at low concentrations, two exchangeable protons correlated with a single nitrogen and the other correlated with the other nitrogen. Thus, **2b** also adopted the expected ADA and DAD tautomeric faces (see Supporting Information). To further demonstrate self-association in the absence of formic acid, an ESI experiment (positive ion mode) was run on compounds **2a** and **2b**. Analysis of **2a** gave evidence of several multimeric sodiated species, (M_{*a*} + Na)⁺ where *a* = 1–6, as well as putative (M_{*b*} + 2Na)²⁺ where *b* = 7, 9, and 11 (see Supporting Information). ESI analysis of **2b** gave several multimeric protonated species (M_{*c*} + H)⁺ where *c* = 4–6, as well as putative (M_{*d*} + 2H)²⁺ where *d* = 8–11.

Likewise, **3** crystallized as colorless plate crystal via slow evaporation of a dilute solution of **3** in 98% formic acid in the presence of methylene chloride. On standing, compound **3** crystallized as formate salt in which the DAD face provides DDD–AD pairing interaction with the thymine-like face due to the protonation of the nitrogen in diaminopyridine ring. Similar to the extended H-bonding network of **2b**, this unique asymmetrical hydrogen-bonding pattern between the pyridinium cation face and the thymine-like face mediated by formate anion, afforded formation of a zigzagged hydrogen-bonded molecular ribbon association. Extension of the unit cell indicated a formate-ion mediated cocrystal as shown in Figure 5A,B.

Significance and Conclusions

This work is, to the best of our knowledge, the first report of high-resolution X-ray structural data for supramolecular solids derived from three self-complementary monomers capable of DAD–ADA H-bonding recognition whose compositions and syntheses have not been known. In the case of compound **1**, four different H-bonded networks cocrystallize to exemplify the microscopic diversity of such DAD–ADA hydrogen bonds that assume different dihedral angles of considerable variance within the same crystal lattice. The observation of such variability in the crystal lattice may have implications for the design of melamine-barbituric/cyanuric acid based structures that are presumed to be rigid and planar but may indeed be more polymorphic or flexible than thought.

In the case of compounds **2b** and **3**, no crystals could be grown in our hands that would have suggested direct association, and the only lattices that could be formed were obtained in the presence of formate. For **2b** we obtained a formate-bridged lattice of an absolutely flattened array that is not actually a DAD–ADA H-bonded lattice but rather a DDD motif interfaced with a DA–AD interaction mediated by formate anion in which the alkyl tails of **2b** were in the same side of the formed linear ribbon. For **3** we obtained a formate-bridged network in which the alkyl tails of **3** were on the opposite sides of the zigzagged ribbon. In this case, we observed a DDD–D H-bonding motif of diaminopurine face aligned with an ADA H-bonding pattern of thymine face mediated by AA H-bonding motif of formate anion.

In no case did we observe rosette-like structures for any of the heterocycles described herein. Taken together, these observations are consistent with the generally accepted relative weakness of the DAD–ADA H-bonding scheme compared to the isosteric DDA–AAD scheme. It is perhaps not surprising that a crystal structure of a DAD–ADA H-bonded supramolecular solid has remained elusive until now.

Not only are these the first crystal structures of compounds with both ADA and DAD faces, but also these structures are featured herein as absolute proof of the constitutional connectivity of three unique J_{AT}-base compositions which have not been previously reported in any form. Such characterization is important if one is to contemplate their future use in developing oligomers and bioconjugates capable of DNA and RNA duplex recognition. In that regard, whereas **1** crystallized nicely with the expected H-bonded tautomers characteristic of A–T base pairs, **2b** and **3** could only be crystallized from 98% formic acid (pH ~ 2) as formate salts. Nevertheless, it is unlikely that at physiological pH (7.4) compounds **2b** or **3** will remain

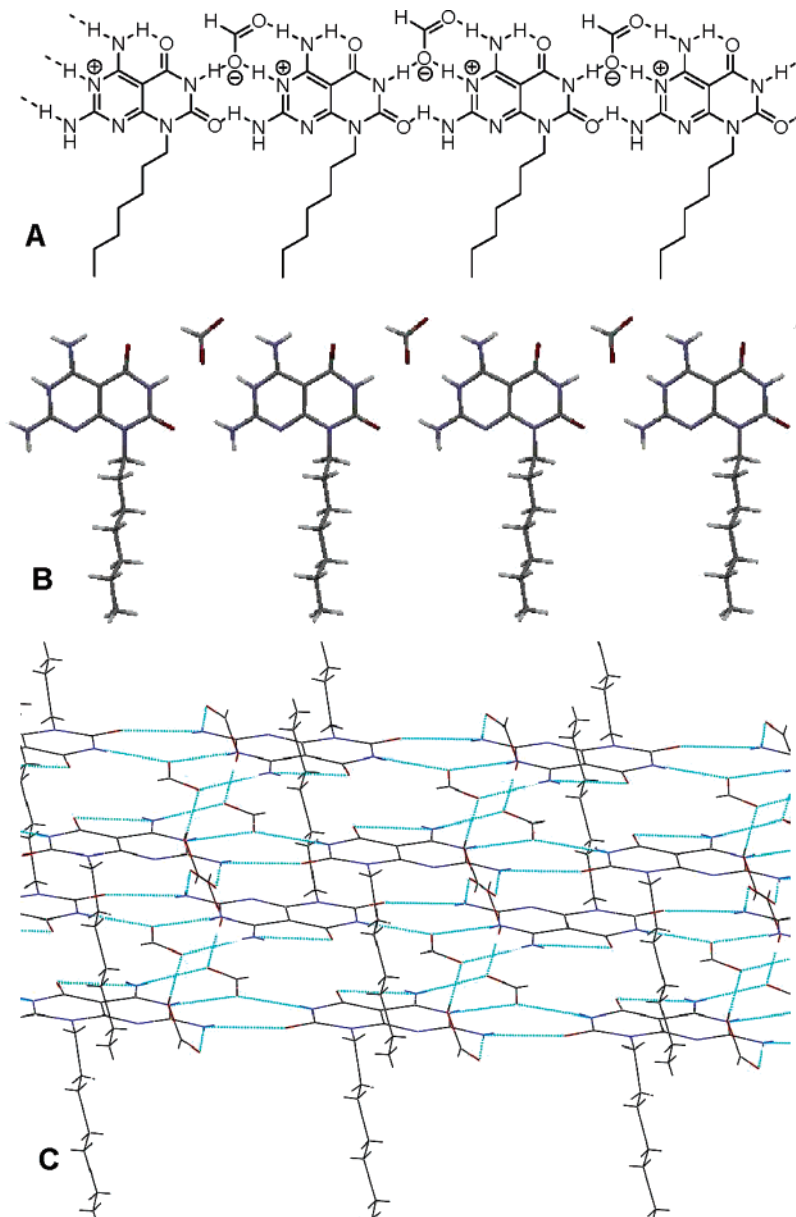


FIGURE 4. (A) Scheme of formate anion bridging the array. (B) X-ray single-crystal structure of supramolecular ribbon of **2b**. (C) The extended structure with interlattice formate bridges.

protonated as formate salts (pK_a 's of diaminopyrimidines, diaminopyridines ~ 5.5) and thus should favor the intended H-bonding recognition patterns as seen for compound **1**, and as confirmed independently by solution phase $^{15}\text{H}-^1\text{H}$ HSQC NMR (**2b**) and by ESI (**2a** and **2b**). On the basis of the similarity between the chemical shifts of **2b** and **3** in the ^1H NMR spectra, along with the structural proof of **3** afforded by X-ray crystallography, we did not further investigate **3** by $^{15}\text{H}-^1\text{H}$ HSQC NMR.

The potential for using J-bases to recognize both Watson-Crick base pairs (GC and AT), and thus any DNA sequence, is an attractive idea that has yet to be fully elaborated. Curiously, despite several previous reports of J_{GC} -bases, the potential for GC base pair recognition has never been investigated. This may be due to (i) an inability to cleanly monitor simultaneous recognition of monomeric G and monomeric C in CDCl_3 against a backdrop of both the self-association of the J_{GC} -base and an independent association of monomeric G with monomeric C,

or (ii) difficulties in preparing soluble oligomers of J_{GC} that will have the suitable length and consequent energetics to permit stable recognition of stretches of nucleic acid sequences.

If such a strategy is to be fully realized, it will necessarily require the synthesis and definitive structural proof of a J_{AT} -base (e.g., **2b**, **3**), as reported herein, that is isosteric for, and which may be used in conjunction with previously reported J_{GC} -bases. The robust syntheses of **2a**, **2b**, and **3** extend the repertoire for using this shape-class of J-bases in the context of an oligomeric scaffold (e.g., PNA, ODN) to potentially recognize any nucleic acid sequence.⁵⁷ Although to date there is no analogous J_{GC} -base corresponding to **1**, such is also readily envisioned to provide for a different shape-class of J_{AT} and J_{GC} bases. The DNA recognition properties of the heterocycles reported herein await full investigation, along with the same for J_{GC} heterocycles.

(57) Dervan, P. B. *Bioorg. Med. Chem.* **2001**, *9*, 2215–2235.

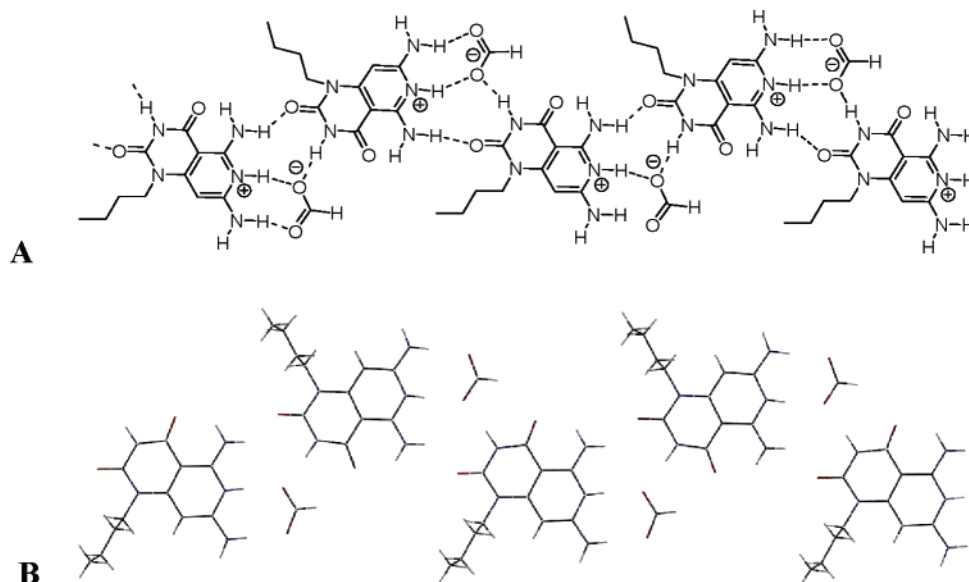


FIGURE 5. (A) Scheme of formate anion bridging the hydrogen bonded array of **3**. (B) X-ray single-crystal structure of supramolecular crinkled ribbon of **3** with formate bridging.

Although alkylated monomers such as **1**, **2b**, and **3** are rather insoluble in water and thus unlikely to find immediate application for DNA or RNA recognition, solubility itself is a complicated issue and the lack thereof in water can be used advantageously to enforce H-bonds in an aqueous medium. For example, both guanine and guanosine are very insoluble in water, yet when properly oligomerized on a water-soluble backbone (e.g., deoxyribosephosphodiester), find use in DNA recognition and nanostructured architectures.⁵⁸ The synthetic routes we report herein should enable a diverse functionalization of $J_{AT}1-3$ for use in bioconjugation and oligomerization. Although at this juncture we have not reported on the synthesis of a derivative that can be oligomerized, such is easily contemplated by using suitably protected (e.g., N_{α} Boc-COOtBu) lysine instead of an alkylamine.

In terms of targeting DNA, J-base target recognition may be complicated by self-association.⁴³ Nonetheless, the formation of hexameric J-base rosettes will be a fifth or possibly sixth order process whereas duplex DNA recognition will be first or second order. As such, low concentrations may be identified to kinetically disfavor higher order self-associated structures and favor duplex formation. That notwithstanding, self-association by ligands designed to target DNA and RNA is neither a new phenomenon nor a reason not to contemplate their use: G-rich oligonucleotides offer high T_m 's with respect to target recognition, yet form self-associated G-quartets in competition with target strand recognition.

Obviously, the other edge of this sword is self-association, which underlies the design of nanostructured assemblies unrelated to DNA recognition. Hexameric rosettes offer interesting properties unto themselves as underscored in a recent report of a hexameric rosette comprising three monomeric deoxyriboseylbarbituric acids and three monomeric deoxyriboseyl-triaminopyrimidines.⁵⁹ It will be interesting to see if two J_{GC} bases which sandwich a J_{AT} base (e.g., $J_{GC}-J_{AT}-J_{GC}$) can enforce a

rosette structure on an internal J_{AT} base that clearly has crystallized out as a tape.

The syntheses presented herein will enable us, and others, to evaluate the properties of self-association, nanostructured assembly, and DNA and RNA recognition. As AT-rich sequences are found at critical regions of both ribozymes and DNA promoters, properly functionalized J_{AT} -bases that recognize such sequences may prove useful for studying the biological processes governed by these sequences. Such recognition will be reported in due time.

Experimental Section

General experimental procedures and methods are given in the Supporting Information.

(Z)-2-Cyano-3-ethoxyacrylethyl carbamate (5). A stirring mixture of *N*-cyanoacetylurethane, **4** (1.56 g, 10 mmol), triethyl orthoformate (1.64 mL, 10 mmol), and acetic anhydride (4 mL) was refluxed at 110 °C for 45 min. The reaction mixture was then allowed to cool to room temperature. The colorless crystals of product were filtered and washed with light petroleum ether (20 mL) and diethyl ether (5 mL) (yield 95%). ¹H NMR (300 MHz, CDCl₃, 25 °C) δ = 1.24 (t, J = 7.14 Hz, 3H, CH₃), 1.38 (t, J = 7.14 Hz, 3H, CH₃), 4.17 (q, J = 7.14 Hz, 2H, CH₂), 4.36 (q, J = 7.14 Hz, 2H, CH₂), 7.91 (br s, 1H, NH), 8.17 (s, 1H, CH). ¹³C NMR (300 MHz, CDCl₃) δ = 14.2, 15.3, 62.5, 74.7, 81.5, 87.0, 104.7, 113.3, 150.1, 159.2, 161.3, 174.2. ESI-MS (m/z) 235 (M + Na)⁺. HRMS (ESI⁺) calcd for C₉H₁₂N₂O₄Na 235.0695, found 235.0697.

1-Butyl-1,2,3,4-tetrahydro-2,4-dioxypyrimidine-5-carbonitrile (6). To a stirring solution of **5** (2.12 g, 10mmol) in water (10 mL) was added butyl amine (0.99 mL, 10mmol), and the reaction mixture was heated at 90 °C for 25 min. The reaction mixture was then allowed to cool to room temperature and acidified by 5 N HCl. The colorless crystals were filtered and washed with cold water (10 mL). (Colorless crystals recrystallized from water, yield 93%.) ¹H NMR (300 MHz, *d*₆-DMSO, 25 °C) δ = 0.87 (t, J = 7.36 Hz, 3H, CH₃), 1.22–1.30 (m, 2H, CH₂), 1.55–1.60 (m, 2H, CH₂), 3.70 (t, J = 7.32 Hz, 2H, CH₂), 8.69 (s, 1H, CH), 11.94 (br s, 1H, NH). ¹³C NMR (300 MHz, *d*₆-DMSO, 25 °C) δ = 13.5, 19.0, 30.3, 48.6, 87.3, 113.9, 114.4, 149.6, 154.7, 160.6. ESI-MS (m/z) 216 (M + Na)⁺. HRMS (ESI⁺) calcd for C₉H₁₁N₃O₂Na 216.0749, found 216.0751.

(58) Seeman, N. *Acc. Chem. Res.* **1997**, *30*, 357–363.

(59) Rakotonradany, F.; Palmer, A.; Toader, V.; Chen, B.; Whitehead, M.; Sleiman, H. *Chem. Commun.* **2005**, 5441–5443.

5-(4,6-Diamino-1,3,5-triazin-2-yl)-1-butylpyrimidine-2,4(1H,3H)-dione (1). A stirring mixture of cyanouracil, **6** (0.97 g, 5 mmol), dicyandiamide (0.46 g, 5.5 mmol), and powdered potassium hydroxide (0.61 g, 11 mmol) in dry DMSO (5 mL) was heated at 100 °C for 5 h. The reaction mixture was then allowed to cool to room temperature, and water (20 mL) was added. The formed solution was acidified by 5 N HCl, and the suspended solid product was filtered and rinsed with water (25 mL) and diethylether (50 mL) to afford pure product **1** (white powder, yield, 80%). ¹H NMR (300 MHz, *d*₆-DMSO) δ = 0.89 (t, *J* = 7.41 Hz, 3H, CH₃), 1.24–1.32 (m, 2H, CH₂), 1.55–1.60 (m, 2H, CH₂), 3.73 (t, *J* = 7.3 Hz, 2H, N–CH₂), 6.69 (br s, 4H, NH₂), 8.15 (s, 1H, CH), 11.98 (br s, 1H, NH). ¹³C NMR (400 MHz, *d*₆-DMSO, 25 °C) δ = 13.6, 19.1, 30.7, 47.6, 139.7, 147.3, 150.4, 160.6, 166.9, 168.3. HRMS (ESI⁺) calcd for C₁₁H₁₆N₇O₂ 278.1365, found 278.1366.

Potassium 2-Cyano-3-(ethoxycarbonylamino)-3-oxoprop-1-ene-1,1-bis-thiolate (7). Compound **4** (1.56 g, 10 mmol) and powdered potassium carbonate (1.38 g, 10 mmol) in dry DMF (25 mL) was vigorously stirred at room temperature for 2 h. Carbon disulfide (1.3 mL, 20 mmol) was added all at once to the suspension, and stirring continued for 4 h. Absolute ethanol (100 mL) was added to the mixture, and the precipitate that formed was filtered and washed with diethyl ether (150 mL), then dried under reduced pressure (pale yellow powder, yield 95%). ¹H NMR (400 MHz, *d*₆-DMSO, 25 °C, TMS) δ = 14.9 (s, 1H, NH), 1.1 (t, *J* = 13 Hz, 3H; CH₃), 4 (q, *J* = 7 Hz, 2H; CH₂). ¹³C NMR (400 MHz, *d*₆-DMSO, 25 °C, TMS) δ = 14.5, 59.5, 97.5, 125.6, 152.4, 164.9, 222.1. ESI-MS (*m/z*) 308 (M⁺). HRMS (ESI) *m/z* calcd for C₇H₇N₂O₃S₂ K₂ 308.9172, found 308.9171.

2-Cyano-3,3-bis (methylthio)acrylethyl carbamate (8). A solution of **7** (3.08 g, 10 mmol) in a water–acetonitrile (40 mL, 7:3) mixture was stirred at room temperature. Methyl iodide (1.3 mL, 22 mmol) in 10 mL acetonitrile was added dropwise to the solution, and the mixture was stirred for 0.5 h at room temperature. The flask was fitted with a reflux condenser, and the reaction mixture was heated under reflux at 95 °C for 3 h. The reaction mixture was then allowed to cool to room temperature and concentrated to 25 mL under reduced pressure with a rotary evaporator. The product was extracted with ethyl acetate (3 × 50 mL). Combined organic phases were washed with brine (100 mL), dried over sodium sulfate, and concentrated on a rotary evaporator to give a viscous oil (pale yellow), which solidified on standing at room temperature under reduced pressure (yield 85%). ¹H NMR (300 MHz, CDCl₃, 25 °C, TMS) δ = 1.27 (t, *J* = 7.1 Hz, 3H, CH₃), 2.62 (s, 3H, S–CH₃), 2.8 (s, 3H, S–CH₃), 4.24 (q, *J* = 7.08 Hz, 2H, CH₂), 7.95 (br s, 1H, NH). ¹³C NMR (300 MHz, CDCl₃, 25 °C, TMS) δ = 14.40, 19.6, 21.1, 29.9, 31.1, 62.8, 98.8, 116.9, 131.3, 150.6, 159.2, 183.0, 188.6. EI-MS (*m/z*) 260 (M⁺). HRMS (EI) *m/z* calcd for C₉H₁₂N₂O₃S₂ 260.02894, found 260.02905.

1-Butyl-1,2,3,4-tetrahydro-6-(methylthio)-2,4 dioxypyrimidine-5-carbonitrile (9a). A solution of **8** (1.3 g, 5 mmol) in absolute ethanol (30 mL) was stirred at room temperature. Butylamine (0.49 mL, 5 mmol) in 10 mL absolute ethanol was added dropwise over a period of 30 min. The flask was fitted with a reflux condenser, and the reaction mixture was heated under reflux at 100 °C for 16 h. The reaction mixture was then allowed to cool to room temperature and the solvent evaporated under reduced pressure with a rotary evaporator. The resulting white powder was recrystallized in ethanol–water (1:1) (yield 83%) (ORTEP diagram and X-ray crystal structure data in the Supporting Information). ¹H NMR (300 MHz, *d*₆-DMSO) δ = 0.95 (t, *J* = 7.3 Hz, 3H, CH₃), 1.33–1.4 (m, 2H, CH₂), 1.58–1.66 (m, 2H, CH₂), 2.92 (s, 3H, S–CH₃), 4.13 (t, *J* = 7.8 Hz, 2H, N–CH₂), 8.6 (br s, 1H, NH). ¹³C NMR (300 MHz, *d*₆-DMSO) δ = 13.5, 19.2, 19.3, 30.3, 46.3, 92.0, 114.6, 149.1, 159.4, 166.3. ESI-MS (*m/z*) 262 (M + Na)⁺. HRMS (ESI⁺) *m/z* calcd for C₁₀H₁₃N₃O₂NaS 262.0626, found 262.0625.

1-Heptyl-6-(methylthio)-2,4-dioxo-1,2,3,4-tetrahydropyrimidine-5-carbonitrile (9b). A solution of **8** (1.3 g, 5 mmol) in absolute ethanol (30 mL) was stirred at room temperature. Hep-

tylamine (0.74 mL, 5 mmol) in 10 mL absolute ethanol was added dropwise over 30 min. The flask was fitted with a reflux condenser, and the reaction mixture was heated under reflux at 100 °C for 16 h. The reaction mixture was then allowed to cool to room temperature and the solvent evaporated under reduced pressure with a rotary evaporator. The resulting white powder was recrystallized in methanol–water (1:1) (yield 87%). ¹H NMR (300 MHz, *d*₆-DMSO) δ = 0.85 (t, *J* = 7.3 Hz, 3H, CH₃), 1.1–1.4 (m, 8H, CH₂), 1.6–1.8 (m, 2H, CH₂), 2.8 (s, 3H, S–CH₃), 4 (t, *J* = 7.8 Hz, 2H, N–CH₂), 8.5 (br s, 1H, NH). ¹³C NMR (300 MHz, *d*₆-DMSO) δ = 14.1, 18.1, 19.26, 22.9, 25.0, 27.9, 28.8, 31.8, 45.7, 92.0, 114.4, 148.5, 159.9, 167.5. ESI-MS (*m/z*) 281 (M⁺). HRMS (ESI⁺) *m/z* calcd for C₁₃H₁₉N₃O₂S 281.1198, found 281.1202.

5,7-Diamino-1-butylpyrimido [4,5-*d*] Pyrimidine-2, 4(1H,3H)-dione (2a). A mixture of guanidinium hydrochloride (0.52 g, 5.5 mmol) and sodium ethoxide (0.37 g, 5.5 mmol) in 5 mL absolute ethanol was heated at 45 °C for 5 min, and a precipitate formed (NaCl) from which the solvent and guanidine free base was filtered off. The filtrate was added to a solution of **9a** (1.2 g, 5 mmol) in absolute ethanol (20 mL). The reaction mixture was heated under reflux at 100 °C for 16 h. The reaction mixture was then allowed to cool to room temperature, and a white precipitate formed, which was filtered and washed with water (2 × 25 mL). The product was then crystallized from formic acid (yield 87%). ¹H NMR (400 MHz, *d*₆-DMSO) δ 0.88 (t, *J* = 7.5 Hz, 3H, CH₃), 1.22–1.31(m, 2H, CH₂), 1.49–1.56 (m, 2H, CH₂), 3.94 (t, *J* = 7.28 Hz, 2H, N–CH₂), 6.86 (br s, 2H, NH₂), 7.40 (br s, 1H, NH), 8.01 (br s, 1H, NH), 11.06 (br s, 1H, NH). ¹³C NMR (600 MHz, *d*₆-DMSO) δ = 13.8, 19.5, 29.6, 48.6, 82.9, 150.4, 159.4, 162.3, 163.6, 163.7. ESI-MS (*m/z*) 251 (M + H)⁺. HRMS (EI) *m/z* calcd for C₁₀H₁₅N₆O₂ 251.1256, found 251.1258.

5,7-Diamino-1-heptylpyrimido[4,5-*d*]pyrimidine-2,4(1H,3H)-dione (2b). A mixture of guanidinium hydrochloride (0.52 g, 5.5 mmol) and sodium ethoxide (0.37 g, 5.5 mmol) in 5 mL absolute ethanol was heated at 45 °C for 5 min, and a precipitate formed (NaCl) which was filtered off. The filtrate was added to a solution of **9b** (1.4 g, 5 mmol) in absolute ethanol (20 mL). The reaction mixture was heated under reflux at 100 °C for 16 h. The reaction mixture was then allowed to cool to room temperature, and a white precipitate formed, which was filtered and washed with water (2 × 25 mL). The product was then crystallized from formic acid (yield 85%). ¹H NMR (300 MHz, *d*₆-DMSO, 25 °C, TMS) δ = 11.1 (s, 1H, NH), 8.1(s, 1H, NH), 7.4 (s, 1H, NH), 6.9 (s, 2H, NH₂), 3.9 (t, *J* = 7.28 Hz, 2H, CH₂), 1.5–1.6 (m, 2H, CH₂), 1.2–1.4(m, 8H, CH₂), 0.8 (t, *J* = 6.8 Hz, 3H, CH₃). ¹³C NMR (400 MHz, *d*₆-DMSO) δ = 14.3, 22.2, 26.5, 27.6, 28.9, 31.6, 83.1, 151.8, 159.8, 162.8, 163.4, 164.2. EI-MS (*m/z*) 293 (M + H)⁺. HRMS (EI) *m/z* calcd for C₁₃H₂₁N₆O₂ 293.1647, found 293.1656.

(2-Cyano-3-ethoxy-but-2-enoyl)carbamic Acid Ethyl Ester (10). A stirring mixture of Compound **4** (1.56 g, 10 mmol), triethyl orthoacetate (1.82 mL, 10 mmol), and acetic anhydride (4 mL) was refluxed at 110 °C for 40 min. The reaction mixture was then allowed to cool to room temperature. The colorless crystals of product were filtered and washed with light petroleum ether (20 mL) and cold diethyl ether (5 mL) (yield 90%). ¹H NMR (300 MHz, CDCl₃, 25 °C) δ = 1.27 (t, *J* = 7.3 Hz, 3H, CH₃), 1.53 (t, *J* = 7.3 Hz, 3H, CH₃), 2.49 (s, 3H, CH₃), 4.2 (q, *J* = 7.3 Hz, 2H, CH₂), 4.39 (q, *J* = 7.3 Hz, 2H, CH₂), 9.14 (br s, 1H, NH). ¹³C NMR (300 MHz, CDCl₃) δ 15.2, 15.6, 19.9, 62.5, 69.9, 93.5, 118.0, 152.3, 160.1, 178.2. ESI-MS (*m/z*) 235 (M + Na)⁺. HRMS (ESI⁺) calcd for C₉H₁₂N₂O₄Na 235.0695, found 235.0697.

1-Butyl-6-methyl-2,4-dioxo-1,2,3,4-tetrahydro-pyrimidine-5-carbonitrile (11). To a stirring solution of **10** (2.26 g, 10mmol) in water (10 mL) was added butyl amine (0.99 mL, 10mmol), and the reaction mixture was heated at 90 °C for 20 min. The reaction mixture was then allowed to cool to room temperature and acidified to pH 5 by the addition of 5 N HCl. The colorless crystals were filtered and washed with cold water (10 mL) and cold diethyl ether (10 mL). Colorless crystals were recrystallized from water–

methanol (1.87 g, yield 91%). ^1H NMR (400 MHz, d_6 -DMSO, 25 °C) δ = 0.99 (t, J = 7.6 Hz, 3H, CH₃), 1.36–1.45 (m, 2H, CH₂), 1.61–1.70 (m, 2H, CH₂), 2.61 (s, 3H, CH₃), 3.9 (t, J = 7.6 Hz, 2H, CH₂), 9.92 (br s, 1H, NH). ^{13}C NMR (400 MHz, d_6 -DMSO, 25 °C) δ = 13.8, 19.6, 20.1, 30.7, 46.1, 90.6, 113.9, 149.6, 159.8, 163.5. ESI-MS (m/z) 208 (M + H)⁺. HRMS (ESI⁺) calcd for C₁₀H₁₄N₃O₂ 208.1086, found 208.1088.

5-Amino-1-butyl-7-thioxo-1,7-dihydro-thiopyrano[4,3-*d*]pyrimidine-2,4-dione (12). To a stirring solution of **11** (2.07 g, 10 mmol) in dry THF (100 mL) was added 35 mmol of potassium *t*-butoxide. The reaction mixture was stirred for 10 min at room temperature followed by dropwise addition of carbon disulfide (25 mmol, 1.6 mL) in THF (10 mL) over period of 10 min. The reaction mixture was stirred vigorously at room temperature until full conversion of starting material (3 h). Upon completion, the solvent was evaporated under reduced pressure. The crude product was dissolved in water (30 mL), and the solution was acidified to pH 5 using glacial acetic acid. The orange precipitate was filtered off and washed with petroleum ether (10 mL) and cold diethyl ether (10 mL). Further purification was obtained by reprecipitating in methanol (2.52 g, yield 89%). Single orange crystals for X-ray analysis were obtained from acetonitrile. ^1H NMR (300 MHz, d_6 -DMSO, 25 °C) δ = 0.94 (t, J = 7.5 Hz, 3H, CH₃), 1.3–1.38 (m, 2H, CH₂), 1.48–1.56 (m, 2H, CH₂), 3.94 (t, J = 7.5 Hz, 2H, CH₂), 6.73 (s, 1H, CH), 9.84 (br s, 1H, NH), 10.57 (br s, 1H, NH), 11.65 (br s, 1H, NH). ^{13}C NMR (300 MHz, d_6 -DMSO, 25 °C) δ = 15.1, 20.8, 30.3, 44.5, 92.9, 111.3, 151.0, 151.3, 163.9, 173.5, 188.7. ESI-MS (m/z) 282 (M)⁻. HRMS (ESI⁻) calcd for C₁₁H₁₂N₃O₂S₂ 282.0371, found 282.0374.

5-Amino-1-butyl-7-thioxo-6,7-dihydro-1H-pyrido[4,3-*d*]pyrimidine-2,4-dione (13). Compound **12** (0.89 g, 3 mmol) and 30% ammonium hydroxide (30 mL) were placed in a 150 mL Teflon-sealed thick-walled glass tube equipped with a magnetic stirrer and was heated while stirring to 100 °C (12 h) (Caution! use blast shield). The mixture was cooled to room temperature, and the excess ammonia was evaporated under reduced pressure. The formed tan precipitate was filtered off and washed with water (10 mL) and cold diethyl ether (20 mL) (0.74 g, yield 93%, tan powder). A single crystal for X-ray crystallography analysis was obtained by using 98% formic acid as crystallization solvent. ^1H NMR (300 MHz, d_6 -DMSO, 25 °C) δ = 0.9 (t, J = 7.26 Hz, 3H, CH₃), 1.25–1.33 (m, 2H, CH₂), 1.43–1.61 (m, 2H, CH₂), 3.82 (t, J = 7.32 Hz, 2H, CH₂), 6.23 (s, 1H, CH), 7.1 (br s, 1H, NH), 8.35 (br s, 1H, NH), 11.33 (br s, 1H, NH), 12 (br s, 1H, NH). ^{13}C NMR (300 MHz, d_6 -DMSO, 25 °C) δ = 14.0, 15.12, 20.8, 30.3, 43.3, 91.4, 94.5, 150.1, 151.5, 160.5, 164.7, 167.1. ESI-MS (m/z) 267 (M + H)⁺. HRMS (ESI⁺) calcd for C₁₁H₁₅N₄O₂S 267.0916, found 267.0914.

5-Amino-1-butyl-7-methylsulfonyl-1H-pyrido[4,3-*d*]pyrimidine-2,4-dione (14). Compound **13** (2.66 g, 10 mmol) was added to an aqueous solution of NaOH (2.4%, 50 mL). The reaction mixture was stirred for 5 min at room temperature followed by dropwise addition of methyl iodide (10 mmol, 0.62 mL) over 3 min. The reaction mixture was stirred at room temperature (1.5 h); upon completion of reaction, the mixture was acidified to pH 6 by dilute HCl and the formed white precipitate filtered off and washed with water (20 mL). Further purification was obtained by reprecipitating in methanol (2.65 g, yield 90%), forming white powder. ^1H NMR (400 MHz, CDCl₃, 25 °C) δ = 1.01 (t, J = 7.6 Hz, 3H, CH₃), 1.39–1.48 (m, 2H, CH₂), 1.62–1.70 (m, 2H, CH₂), 2.54 (s, 3H, CH₃), 3.93 (t, J = 7.6 Hz, 2H, CH₂), 5.52 (br s, 1H, NH), 6.17 (s,

1H, CH), 8.35 (br s, 1H, NH), 8.54 (br s, 1H, NH). ^{13}C NMR (400 MHz, d_6 -DMSO, 25 °C) δ = 14.0, 15.1, 20.8, 30.2, 43.3, 91.4, 94.5, 150.1, 151.5, 160.5, 164.7, 167.1. ESI-MS (m/z) 281 (M + H)⁺. HRMS (ESI⁺) calcd for C₁₂H₁₇N₄O₂S 281.1072, found 281.1071.

5-Amino-1-butyl-7-methanesulfonyl-1H-pyrido[4,3-*d*]pyrimidine-2,4-dione (15). **Method A.** Compound **14** (5 mmol, 1.4 g) was dissolved in formic acid 88% (10 mL), and hydrogen peroxide 30% (15 mmol, 1.7 mL) was added dropwise to the solution at 0 °C over 5 min. The reaction mixture was stirred for 5 h at room temperature. Upon completion, the solvent was evaporated under reduced pressure. The crude product was washed with water (10 mL) and diethyl ether (5 mL) to afford 1.48 g (95%) of a pale yellow solid.

Method B. Compound **14** (5 mmol, 1.4 g) was dissolved in chloroform (50 mL) along with 3-chloroperoxybenzoic acid 77% (15 mmol, 2.5 g). The reaction mixture was stirred for 4 h at room temperature. Upon completion, the solvent was evaporated under reduced pressure. The crude product was washed with diethyl ether (50 mL) to afford 1.2 g (81%) of a pale yellow solid. ^1H NMR (400 MHz, d_6 -DMSO, 25 °C) δ = 0.92 (t, J = 7.6 Hz, 3H, CH₃), 1.3–1.39 (m, 2H, CH₂), 1.52–1.59 (m, 2H, CH₂), 3.24 (s, 3H, CH₃), 3.97 (t, J = 7.6 Hz, 2H, CH₂), 6.9 (s, 1H, CH), 7.97 (br s, 1H, NH), 8.41 (br s, 1H, NH), 11.85 (br s, 1H, NH). ^{13}C NMR (400 MHz, d_6 -DMSO, 25 °C) δ = 15.0, 20.7, 30.3, 40.7, 95.3, 96.7, 151.2, 152.4, 161.3, 162.2, 164.5. EI-MS (m/z) 312 (M). HRMS (EI) calcd for C₁₂H₁₆N₄O₄S 312.08923, found 312.08917.

5,7-Diamino-1-butyl-1H-pyrido[4,3-*d*]pyrimidine-2,4-dione (3). Compound **15** (2 mmol, 0.62 g) was suspended in ammonia in methanol (7 N, 10 mL), and the mixture was placed in a 150 mL Teflon-sealed thick-walled glass tube equipped with a magnetic stirrer and heated while stirring to 100 °C (24 h) (Caution! use blast shield). The mixture was cooled to room temperature, and the excess ammonia was evaporated under reduced pressure. The precipitate was washed with water, methanol, and diethyl ether to afford 0.45 g (92%) of a white solid. ^1H NMR (400 MHz, d_6 -DMSO, 25 °C) δ = 0.93 (t, J = 7.6 Hz, 3H, CH₃), 1.29–1.38 (m, 2H, CH₂), 1.48–1.58 (m, 2H, CH₂), 3.75 (t, J = 7.6 Hz, 2H, CH₂), 5.47 (s, 1H, CH), 6.45 (br s, 2H, NH₂), 6.72 (br s, 1H, NH), 8.09 (br s, 1H, NH), 10.79 (br s, 1H, NH). ^{13}C NMR (400 MHz, d_6 -DMSO, 25 °C) δ = 13.7, 19.5, 28.6, 41.7, 79.9, 84.8, 149.2, 150.3, 160.7, 162.5, 162.6. ESI-MS (m/z) 248 (M)⁻. HRMS (ESI⁻) calcd for C₁₁H₁₄N₅O₂ 248.1147, found 248.1149.

Acknowledgment. This work was supported by NSERC. D.M.P. is the recipient of a Junior Career Scholar Award of the Michael Smith Foundation for Health Research in British Columbia, and A.A. is the recipient of a Gladys Estella Laird predoctoral fellowship. We thank Dr. Nick Burlinson for instruction on ^{15}N NMR experiments, Dr. Marcel Hollenstein for T_m Analysis of the Interaction of DNA with **2b**, and Professor Marco A. Ciufolini for critical reading of this manuscript.

Supporting Information Available: ^1H and ^{13}C NMR spectra, ^1H – ^{15}N HSQC data, and CIF files of the X-ray structures. This material is available free of charge via the Internet at <http://pubs.acs.org>.

JO061840K